Analysis of Welding Shrinkage

A simplified approach to estimating welding shrinkage assumes the plate being welded contains a thermoelastoplastic zone and a fully elastic zone

BY N. R. MANDAL and C. V. N. SUNDAR

ABSTRACT. The problems of distortion, residual stresses and reduced strength of structure in and around a welded joint are of major concern in the shipbuilding industry and in other similar manufacturing industries. The present paper deals with the theoretical analysis of transverse shrinkage in a welded butt joint. The mathematical model used in this analysis is based on the assumption that the plate undergoing welding is made up of a thermoelastoplastic zone and a fully elastic zone. The analysis provides a simplified approach for estimating welding shrinkage.

Introduction

Welding is the most frequently used metal joining method, and the complex problem of welding distortion is an obstacle that must be overcome. During the heating and cooling cycles while welding, thermal strains occur in the metal and the base metal regions near the weld. The strains produced during heating are accompanied by plastic upsetting. The stresses resulting from the strains combine and react to produce internal forces, causing shrinkage of the material. Depending on the shrinkage pattern, various structural deformations such as bending, buckling and rotation take place. These deformations are referred to as welding distortions.

This investigation aims at finding the transverse shrinkage in a welded butt joint between two plates having equal thickness. Several investigators have worked on welding distortion and have suggested different methodologies to estimate these shrinkages. An analytical model to predict the transverse shrinkage has been presented by Gupta (Ref. 1).

The effect of the physical and mechanical properties of metals on distortion has been reported (Ref. 2). During the heating and cooling cycles of a welding process, many factors affect shrinkage of the metal, making accurate predictions of distortion complex and difficult. The physical and mechanical properties of the metal that affect the degree of distortion change with the application of heat. As the temperature of the weld area increases, the yield strength, the modulus of elasticity and the thermal conductivity of the steel decrease, whereas the specific heat and the coefficient of thermal expansion increase.

To accommodate the shrinkage of a welded joint on cooling, stresses must reach the yield strength of the weld metal. The higher the yield strength, the higher the residual stress that can act to distort the assembly. Conversely, distortion in lower strength materials is less likely.

The modulus of elasticity is a measure of the stiffness of a material. A higher modulus material is more likely to resist distortion.

Thermal conductivity gives a measure of the ease of heat flow through a material. Metals with low thermal conductivity do not dissipate heat rapidly, and a steep temperature gradient results. Hence the shrinkage effect in the weld and in the adjacent plate increases.

The amount of expansion or contraction a metal will undergo during a heating or a cooling cycle depends on the coefficient of thermal expansion. The possibility of distortion will be larger in metals having a higher coefficient of thermal expansion because they are expected to experience higher shrinkage during cooling of the weld metal and the adjacent metal.

Masubuchi has dealt with various types and causes of welding distortions (Ref. 3). Various empirical relations have been presented for estimating different types of welding distortions (Refs. 4, 5).

Apart from these empirical means, various other methodologies based mainly on the finite element method (FEM) have been used by investigators to predict welding distortions (Refs. 6–8). The computational requirements (long CPU times) of these numerical methods for thermoelastoplastic analysis make the solutions very expensive. In this work, a simplified approach based on a logical sequence of thermally induced distortions has been suggested for estimation of transverse shrinkage of welded steel panels.

A mathematical model for predicting transverse shrinkage due to welding has been developed by assuming near and far field zones (Ref. 9). The near field has been assumed to extend from the weld line to a

KEY WORDS

Distortion
Shrinkage
Weld in a Butt Joint
Near Field
Far Field
Temperature Distribution
Heat Conduction
Heat Flow
Quasi-Stationary State

N. R. MANDAL is an Assistant Professor with the Department of Ocean Engineering and Naval Architecture, Indian Institute of Technology, Kharagpur, India. C. V. N. SUNDAR is a Postgraduate Student with the Department of Ocean Engineering and Naval Architecture, Indian Institute of Technology, Kharagpur, India.

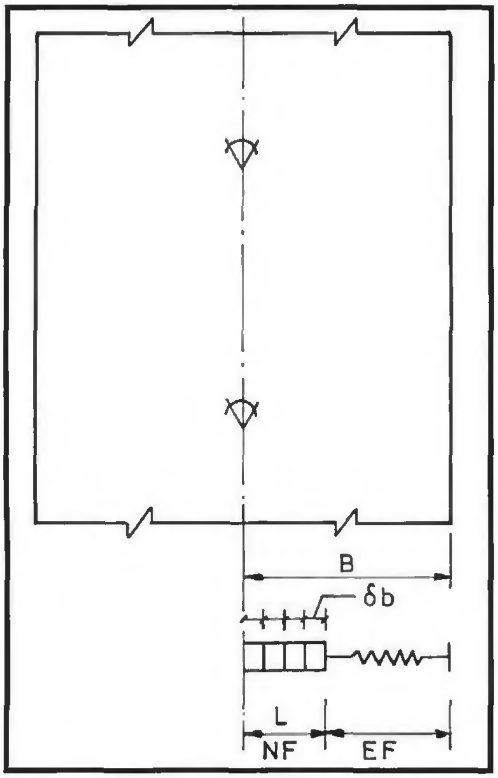

Fig. 1 — Near field/far field model of the plate.

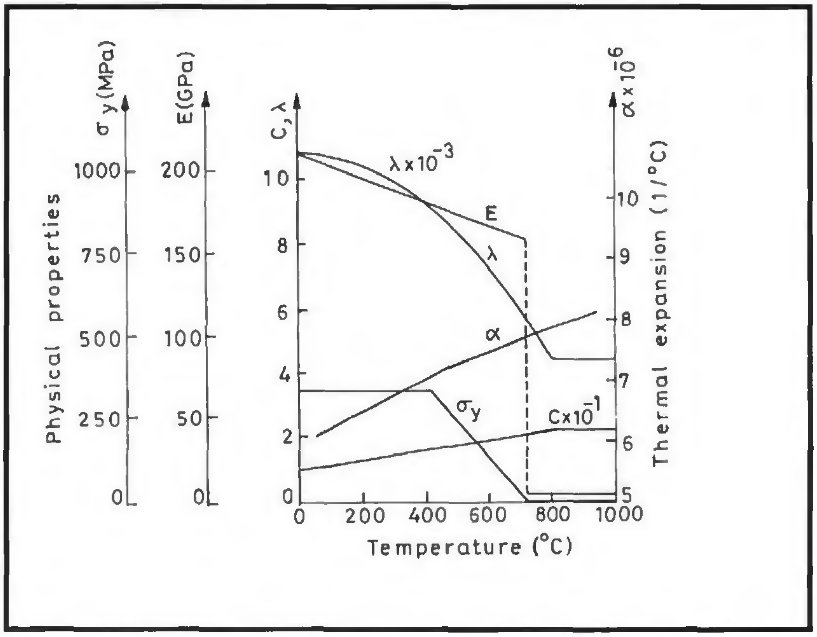

Fig. 2 — Temperature-dependent properties.

distance where the peak temperature attained is 350°C, and the rest of the plate is considered to comprise the far field. The plastic deformations are expected to occur only in the near field, whereas the far field behaves elastically throughout the heating and cooling cycles.

The temperature field associated with the moving welding arc has been solved by assuming a quasi-stationary state (Ref. 10) and using a temperature-dependent specific heat and the thermal conductivity (Ref. 11). The residual shrinkage considering a temperature-dependent coefficient of thermal expansion (Ref. 12) has been calculated by subdividing the near field into finite strips.

Theoretical Analysis of Welding Shrinkage

The effective heat from the electric arc is assumed to be distributed equally in both plates. Therefore, only one plate will be considered for the distortion analysis.

The mathematical model is based on the assumption that the plate is made of a thermoelastoplastic zone and a fully elastic zone. The former, which is near the welded joint, has been termed the near field and the rest, which remains elastic during the heating and cooling phases, is termed the far field.

Hence, the plate undergoing welding can be modeled as a combination of a thermoelastoplastic bar and an elastic spring — Fig. 1.

Assumptions

1) The plates being welded are assumed to be sufficiently long to consider a quasi-stationary state of heat conduction.

2) The yield stress and the modulus of elasticity are assumed to be varying linearly with temperature:

$$\sigma_y = \sigma_{y0}\left(1 - \frac{T}{T_m}\right) \tag{1}$$

$$E = E_0\left(1 - \frac{T}{T_m}\right) \tag{2}$$

A more realistic variation of these properties with temperature is shown in Fig. 2 (Ref. 12). The above-mentioned simplification, which closely approximates the actual case, has been performed to obtain analytical expressions for the estimation of welding shrinkage.

3) The coefficient of thermal expansion is assumed to be linearly dependent on temperature, which is a close approximation of the actual case — Fig. 2.

4) The model assumes that no hardening takes place in the bar.

Until the thermoelastoplastic bar (*i.e.*, the near field zone) reaches the plastic state, the strain is given by

$$\varepsilon = \varepsilon^e + \varepsilon^{th}$$

$$\text{also} \quad \varepsilon = \frac{\delta}{L} \tag{3}$$

where ε^{th} is the thermal strain = $T\alpha$ and T is the difference between the peak temperature and room temperature at any given point in the near field.

$$\text{Now} \quad \varepsilon^e = \frac{-K\delta}{AE}$$

$$\therefore \quad \varepsilon = -\frac{K\delta}{AE} + \alpha T \tag{4}$$

From Equations 3 and 4,

$$\delta = \frac{\alpha L T}{\left(1 + \dfrac{KL}{AE}\right)} \tag{5}$$

Substituting E from Equation 1 into Equation 5,

$$\delta = \frac{\alpha L T}{1 + \dfrac{LKT_m}{AE_0\left(T_m - T\right)}} \tag{6}$$

where K is the equivalent spring constant of the material in the far field. The temperature gradient at the near field boundary being very stiff, the majority of the far field remains at room temperature — Fig.

3. Hence K is considered to be independent of temperature.

Incorporating K_R, Equation 6 can be written as

$$\delta = \frac{(T_m - T)\alpha LT}{T_m(1+K_R)-T} \quad (7)$$

Equation 7 gives the relationship between the displacement temperature and the temperature-dependent Young's modulus for the near field before it attains the plastic state.

By using the force equilibrium, the yield point is determined:

$$\sigma y = \left|\frac{K\delta y}{A}\right| \quad (8)$$

σy_0 is the yield stress at room temperature and is given by

$$\delta y_0 = \left|\frac{K\delta_0}{A}\right| \quad (9)$$

From Equations 1, 8 and 9,

$$\delta y = \pm\delta_0\left(1-\frac{T}{T_m}\right) \quad (10)$$

(+ve for the heating phase; –ve for the cooling phase).

Now, if heating is continued at the same point, the thermoplastic bar, *i.e.*, the near field, will undergo plastic deformation.

The intersection of elastic and plastic processes takes place at T_0, *i.e.*, at T_0 the yield point is encountered for the first time.

Substituting $T = T_0$ in Equations 7 and 10 and then comparing these two equations, one obtains T_0:

$$T_0 = \frac{\delta_0(1+K_R)T_m}{\delta_0 + \alpha T_m L} \quad (11)$$

For the heating phase, δ_0 from Equation 9 is given by

$$\delta_0 = \frac{A\sigma y_0}{K}$$

Substituting this value of δ_0 in Equation 11, one obtains T_0:

$$T_0 = \left(\frac{\sigma y_0(1+K_R)T_m}{\sigma y_0 + \alpha E_0 K_R T_m}\right) \quad (12)$$

During the heating period, with the peak temperature greater than T_0, the shrinkage becomes

$$\delta = \delta_0\left(1-\frac{T}{T_m}\right) \quad \text{for} \quad T_0 < T \le T_m$$

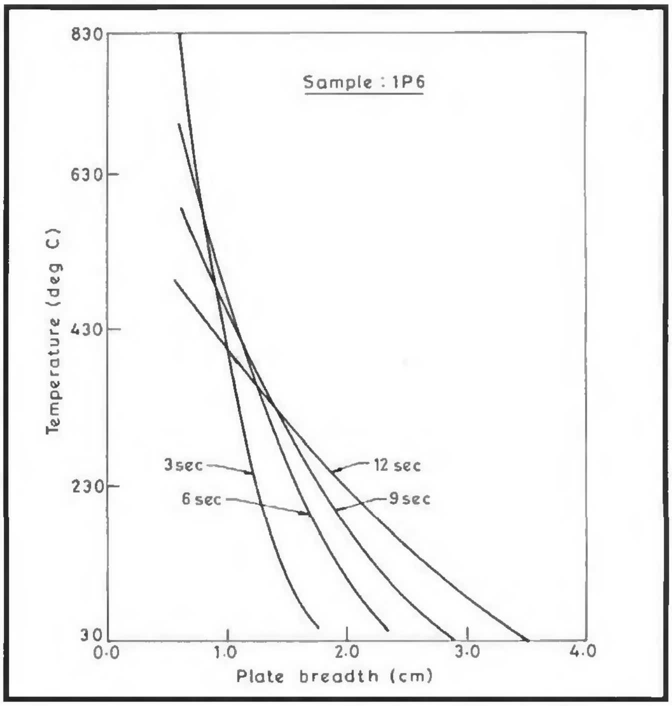

Fig. 3 — Temperature distribution across the breadth of a plate undergoing welding.

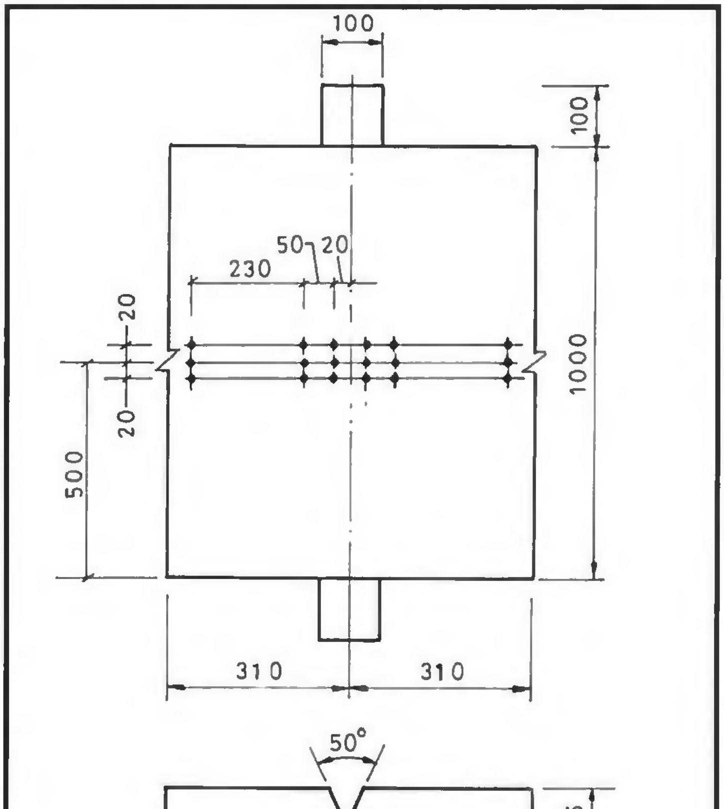

Fig. 4 — MS test sample for shrinkage measurements.

Therefore, the shrinkage at the peak temperature T_p is given by

$$\delta_p = \delta_0\left(1-\frac{T_p}{T_m}\right) \tag{13}$$

When the peak temperature T_p is higher than the yield temperature T_0, plastic deformation is ensured and the residual shrinkage will not be zero.

After the attainment of the peak temperature, the cooling phase begins and is accompanied by elastic unloading.

Before any plasticity occurs while cooling, the incremental strain is given by

$$\Delta\varepsilon = \frac{\delta-\delta_p}{L} = \Delta\varepsilon^e + \Delta\varepsilon^{th} \tag{14}$$

Now

$$\Delta\varepsilon^e = \frac{\sigma-\sigma_p}{E}$$

Taking the values of E and σ from Equations 1 and 2 and considering the value of σ_p to be as follows,

$$\sigma_p = -\frac{K\delta_p}{A}$$

one obtains

$$\Delta\varepsilon^e = -\frac{K\left(\delta-\delta_p\right)T_m}{A\left(T_m-T\right)E_0} \tag{15}$$

The thermal strain increment is given by

$$\Delta\varepsilon^{th} = \alpha\left(T-T_p\right) \tag{16}$$

Substituting Equations 15 and 16 into Equation 14,

$$\delta = \delta_0\left(1-\frac{T_p}{T_m}\right)-\frac{\left(T_m-T\right)\alpha L\left(T_p-T\right)}{T_m\left(1+K_R\right)-T} \tag{17}$$

Equation 17 holds true until the temperature T decreases to a point and the near field attains a yield point; this causes plastic deformation in the other direction, and shrinkage takes place.

At the temperature T_1 (in the cooling cycle) yielding takes place. From Equations 2 and 17 (using a negative sign for the cooling period),

$$-\delta_0\left(1-\frac{T_1}{T_m}\right) = \delta_0\left(1-\frac{T_p}{T_m}\right)-\frac{\left(T_m-T\right)\alpha l\left(T_p-T_1\right)}{T_m\left(1+K_R\right)-T_1}$$

To ensure that plastic deformation takes place during the cooling period, T_1 must be greater than zero. This requires a minimum value of T_p, which is given by

$$T_p \geq \frac{2\delta_0\left(1+K_R\right)T_m}{\delta_0\left(1+K_R\right)+\alpha L T_m} \tag{18}$$

When Equation 18 is satisfied and the temperature falls below T_1, the displacement temperature relation is governed by the following plasticity condition:

$$\delta = -\delta_0\left(1-\frac{T}{T_m}\right) \quad \text{for} \quad 0 < T < T_1 \quad \text{and} \quad dT < 0$$

If the spring stiffness is not high enough to lead the bar into plastic deformation during heating, there will be no residual displacements even though the elastic deformation is not linear

i.e., $\delta_r = 0$ for $K < K_0$

K_0 is the critical value of the spring constant leading the bar into the plastic state at the peak temperature. This can be determined by substituting T_p in place of T_0 in Equation 12 and replacing K_R by K_{R0}:

$$K_R = \frac{\sigma y_0\left(T_m-T_p\right)}{T_m\left(\alpha E_0 T_p-\sigma y_0\right)} \tag{19}$$

Substituting $K_{R0} = LK_0/(AE_0)$ in Equation 19, one obtains the value of K_0 as

$$K_0 = \frac{AE_0\sigma y_0\left(T_m-T_p\right)}{LT_m\left(\alpha E_0 T_p-\sigma y_0\right)} \tag{20}$$

Equation 20 gives the critical value of the spring constant so as to initiate yielding at the peak temperature during heating.

If K is greater than K_0 but not high enough to lead the bar into the plastic state during cooling, the residual distortion in that case can be found by substituting T = 0 in Equation 17:

$$\delta_r = \delta_0\left(1-\frac{T_p}{T_m}\right)-\frac{\alpha L T_p}{1+K_R} \quad \text{for} \quad K_{R0} < K_R < K_R$$

Replacing K_R with K_{R1} in Equation 18 and simplifying, one obtains

$$K_{R1} = \frac{\left(2T_m-T_p\right)\sigma y_0}{\alpha E_0 T_m T_p-\left(2T_m-T_p\right)\sigma y_0} \tag{21}$$

If the spring constant is even higher, *i.e.*, $K_R > K_{R1}$, then the final residual distortion will be obtained by setting T = 0 and replacing δ by δ_r in the following equation:

$$\delta = -\delta_0\left(1-\frac{T}{T_m}\right)$$

$$\text{i.e.,} \quad \delta_r = -\delta_0$$

$$\text{i.e.,} \quad \delta_r = -\frac{\sigma y_0}{E_0 K_R}L \quad \text{for} \quad \Delta \geq \Delta_1 \tag{22}$$

Substituting K_R in Equation 22 with K_{R1} as given in Equation 21, one obtains

$$\delta_{r_{max}} = -\left[\frac{\alpha T_m T_p}{2T_m-T_p}-\frac{\sigma y_0}{E_0}\right]L \tag{23}$$

Equation 23 gives the final shrinkage after the bar has cooled down to room temperature.

The method followed to calculate the residual shrinkage using Equation 23 is stated below.

A user interactive computer program has been written in C language and comprises two modules. Module I calculates the temperature distribution over the plate for the given welding parameters and temperature-dependent metal properties. Based on this temperature distribution, the extent of the near field and far field zones is estimated.

The near field is further subdivided into finite strips. The temperature across the strips is assumed to be constant. It is noted that the calculated residual shrinkage is dependent on the width of the strips. This seems to be justified because the temperature across the width of each strip is assumed to be the same, which in reality is not the case. Analysis of available shrinkage data leads to a correlation between welding heat input, welding speed, plate thickness and width of the strips. The obtained relation between these parameters is given by

$\delta b =$
$-0.898 + 7.402 \times 10^{-4}Q - 6.248 \times 10^{-8}Q^2$
where δb = strip width (cm)
and $Q = \eta vi/st$ (J/cm²)

For calculating shrinkage, a suitable strip width is chosen on the basis of the above relation.

For each strip, depending on its peak

Table 1 — Place Particulars and SAW Parameters

	Plate Dimensions				SAW Parameters		
Sample Identification	length (mm)	breadth (mm)	thickness (mm)	Material	Current (A)	Voltage (V)	Speed (cm/s)
1P6	1000	240	6	MS	520	26	1.80
2P6	1000	240	6	MS	520	28	1.60
3P6	1000	240	6	MS	540	27	1.80
4P6	1000	240	6	MS	440	30	1.83
1P12	1000	240	12	MS	480	32	0.93
E1	12000	3000	16	AH32	1180	33	1.13
E2	12000	3000	19.5	AH32	1230	33	1.05

Table 2 — Comparison of Experimental and Theoretical Shrinkages

	Shrinkage		
Sample Identification	Experimental (mm)	Theoretical (mm)	% Deviation
1P6	0.60	0.626	4.30
2P6	1.02	1.140	11.76
3P6	0.52	0.556	6.90
4P6	0.49	0.508	3.67
1P12	0.26	0.278	6.92
E1	0.80	0.750	6.25
E2	0.80	0.795	0.62

temperature, the distortion is calculated by using Equation 23.

The algebraic sum of the distortion of each strip was taken to obtain the final distortion of the plate.

Experimental Verification

The shrinkage measurements were carried out on mild steel samples welded in a butt joint using submerged arc, one-sided welding — Fig. 4. The plate dimensions and the welding parameters are shown in Table 1. The plates were assembled, tack welded and fitted with run on and run off tabs. The tabs were provided with the same edge details as those of the plates. The welding was carried out from one end to the other.

Lines parallel to the welding line were drawn on the plates before welding, and some predetermined positions on the lines at the middle part of the plates were punch marked. The distance between these lines was measured before and after welding. The transverse shrinkage is obtained from the difference between these measurements over the full width of the plates. Half of this value has been taken as the shrinkage in each of the individual plates. The results are shown in Table 2 for samples 1P6 to 1P12.

Ueda, *et al.*, has carried out measurements of welding shrinkage in AH32 steel (Ref. 11). The plate sizes, welding parameters and measured shrinkages over the middle part of the plates are shown in Tables 1 and 2, samples E1 and E2.

The calculated shrinkages based on the present analysis are given in Table 2 followed by a column indicating the percent deviation of the predicted values from the actual measured ones. The deviations are well within 7%, except for sample 2P6 in which case it is around 12%. This could be due to some measurement error. The other predicted shrinkage values agree quite well with the measured ones. However, there is a tendency to overestimate shrinkage. This can be due to overestimation of the welding heat input. It has been assumed that the arc efficiency is 85%.

Conclusion

The predictions of the degree of shrinkage in ship panels due to welding are of great importance from the point of view of dimensional control. A simple, easy to use mathematical tool will be of great help to the designers to account for the shrinkages taking place during fabrication of various flat plate panels.

The main conclusions derived from the present investigation are as follows:

1) A simple methodology has been developed to predict the transverse shrinkage during welding in a butt joint. A user-interactive software program has been developed based on this methodology.

2) Fairly good agreement between the measured and calculated results has been achieved.

3) These results suggest that the developed PC-based software is quite reliable and can be used as a design tool to account for welding shrinkages in practical cases.

4) The present method, however, has limitations as far as the end shrinkages are concerned. Because the analysis is based on the assumption of a quasi-stationary state, the shrinkage effect at the start and end of welding cannot be estimated. However, in the case of ship panels, the panel dimensions are generally very large, on the order of 8–10 m or more. The extent of transient zones at the start and finish of the weld is very small compared to the length of the whole panel. Hence, this method can be gainfully utilized to predict welding shrinkage in the fabrication of ship panels.

References

1. Gupta, O. P., and De, N. R. 1988. Analysis of Transverse Shrinkage in Restrained and Unrestrained Weld. International Conference on Welding Technology, Sept. 1988, University of Roorkee, India.

2. The Lincoln Electric Company. 1973. *Weldment Distortion, The Procedure Handbook of Arc Welding,* Twelfth ed., The Lincoln Electric Company, Cleveland, Ohio.

3. Masubuchi, K. 1980. *Analysis of Welded Structures, Residual Stresses, Distortion and their Consequences,* Pergamon Press, Oxford and New York.

4. Mandal, N. R., and Bhangale, S. D. 1989. Welding distortion in built-up MS T-sections. *Journal of Welding and Metal Fabrication.*

5. The Welding Institute. 1968. *Control of Distortion in Welded Fabrications,* The Welding Institute, Abington, England.

6. Friedman, E. 1975. Thermo mechanical analysis of the welding process using the finite element method. *Transactions of ASME.*

7. Papazoglou, I., Masubuchi, K., Goncalves, E., Imakita, A. 1982. Residual stresses due to welding: computer aided analysis of their formulation and consequences. *SNAME Transactions* 90: 365-310.

8. Hou, A. A., and Tsai, C. L. 1986. A methodology for analyzing welding distortion of tubular frames. *Proceedings of International Conference on Trends in Welding Research,* Gatlinburg, Tenn.

9. Moshaiov, A., and Song, H. 1990. Near and far field approximation for analysing flame heating and welding. *Journal of Thermal Stresses.*

10. Karlsson, L. 1986. Thermal Stresses in Welding. *Thermal Stresses I,* Ed. by R. B. Hetnarski, Chapter 5, Elsevier Science Publishers B. V.

11. Ueda, Y., *et al.,* 1992. Simulation of welding deformation for precision ship assembling (Report - I). *Transactions JWRI* 21(2).

12. Shin, Y., *et al.* 1992. Determination of residual stresses in thick section weldments. *Welding Journal* 71: 305-s to 312-s.

Symbols Used

E Young's modulus of elasticity of the material at any given temperature T

E_0 Young's modulus of the material at room temperature

F Equivalent spring resistance offered by the material in the far field zone

i Welding current (A)

K Equivalent spring constant of the material in the far field zone (elastic)

K_0 Critical value of the spring constant leading the elastic bar into the plastic state at the peak temperature

L Length of the near field zone

s Welding speed (cm/s)

t Plate thickness (cm)

v Welding voltage (V)

T Temperature at any point within the bar

T_0 Temperature at which the intersec-

tion of the elastic and plastic states of the material takes place in the heating phase

T_m Melting temperature of the material

T_p Peak temperature for a given heat input

T_1 Temperature at which the elastic and plastic states intersect in cooling phase

α Coefficient of thermal expansion of the material

ε Strain in the near field zone before it reaches the plastic state

ε^{th} Thermal strain of the near field zone before it reaches the plastic state

δ Shrinkage in the near field zone at a temperature T

δ_0 Shrinkage in the near field zone at room temperature

δ_p Shrinkage in the near field zone at the peak temperature T_p

δ_y Shrinkage corresponding to the given yield stress of the material

$\Delta\varepsilon$ Incremental strain of the near field zone before it reaches the plastic state in the cooling phase

$\Delta\varepsilon^e$ Incremental elastic strain in the near field zone before it reaches the plastic state in the cooling phase

$\Delta\varepsilon^{th}$ Incremental thermal strain in the near field zone before it reaches the plastic state in the cooling phase

η Arc efficiency

K_R Relative stiffness ratio of the near field zone

K_{R0} Critical relative stiffness leading the bar into the plastic state in the heating phase

K_{R1} Critical relative stiffness leading the bar into the plastic state in the cooling phase